Gold Particles as Templates for the Synthesis of Hollow Polymer Capsules. Control of Capsule Dimensions and Guest Encapsulation

Stella M. Marinakos, James P. Novak, Louis C. Brousseau III, A. Blaine House, Efe M. Edeki, James C. Feldhaus, and Daniel L. Feldheim*

Contribution from the Department of Chemistry, North Carolina State University, Raleigh, North Carolina 27695

Received March 24, 1999

Abstract: A method for synthesizing hollow nanoscopic polypyrrole and poly(*N*-methylpyrrole) capsules is described. The method employs gold nanoparticles as templates for polymer nucleation and growth. Etching the gold leaves a structurally intact hollow polymer capsule with a shell thickness governed by polymerization time (ca. 5 to >100 nm) and a hollow core diameter dictated by the diameter of the template particle (ca. 5−200 nm). Transport rates of gold etchant through the polymer shell to the gold core were found to depend on the oxidation state of the polymer, those rates being a factor of 3 greater for the reduced form of the polymer. We show for the first time that not only is the particle a useful template material but also that it can be employed to deliver guest molecules into the capsule core. For example, ligands attached to the gold surface prior to poly(*N*-methylpyrrole) formation remained trapped inside the hollow capsule following polymer formation and gold etching.

Introduction

The list of potential applications for nanostructured composites and hollow polymeric nanocapsules is large. Drug delivery,[1] cell and enzyme transplantation,[2] contaminated waste removal,[3] gene therapy,[4] and heterogeneous catalysis[5] are perhaps at the top of this list. In response to the growing need for encapsulation materials, several different routes to hollow ceramic and polymeric capsules have been developed over the past few years. For example, dendrimers,[6] block copolymers,[7] vesicles,[8] hydrogels,[9] and template-synthesized microtubules[10] have been synthesized and in some cases shown to be viable encapsulants for catalytic metal clusters, small molecules, or enzymes. A more recent approach to the synthesis of hollow nanocapsules, taken by our group[11] and others,[12] is to employ a micrometer- or nanometer-sized particle as a template from which to grow the capsule shell. Dissolution of the template particle often yields a structurally intact hollow capsule, the inner diameter governed by the diameter of the template (Scheme 1). Hollow silica spheres,[12a] multilayer hybrid silica/polymer capsules,[12b] and our own pyrrole-based polymer capsules[11] are examples of this approach.

In this paper, we show the versatility of our methods for synthesizing hollow polymer nanocapsules. Core diameters from ca. 5 to 200 nm, shell thicknesses from ca. 5 to 100 nm, and multilayers of chemically distinct polymers (e.g., poly(pyrrole)/poly(*N*-methylpyrrole)) are synthesized routinely using these methods. We have also found that transport rates of small molecules into the capsule core are affected by the oxidation state of the conductive polymer, a feature of potential utility in many molecular uptake and release scenarios. Finally, we show for the first time that not only is the particle a useful template material but also it can be employed to deliver guest molecules into the capsule core.

The synthetic methods described below are complementary to those reported by others for several reasons. First, capsule shell thickness is not limited by time-consuming sequential polyelectrolyte deposition cycles. Second, the number of capsules synthesized is not limited by the density of pores in a

* To whom correspondence should be addressed. E-mail: Dan_Feldheim@NCSU.edu.

(1) (a) Langer, R. *Science* **1990**, *249*, 1527. (b) Peppas, N. A.; Langer, R. *Science* **1994**, *263*, 1715. (c) Langer, R. *Acc. Chem. Res.* **1993**, *26*, 537. Gill, I.; Ballesteros, A. *J. Am. Chem. Soc.* **1998**, *120*, 8587. (d) Sahoo, S. K.; De, T. K.; Ghosh, P. K.; Maitra, A. *J. Colloid Interface Sci.* **1998**, *206*, 361. (e) Cohen, S.; Bano, M. C.; Visscher, K. B.; Chow, M.; Allcock, H. R.; Langer, R. *J. Am. Chem. Soc.* **1990**, *112*, 7832. (f) Pathak, C. P.; Sawhney, A. S.; Hubbell, J. A. *J. Am. Chem. Soc.* **1992**, *114*, 8311. (g) Gopferich, A.; Alonso, M. J.; Langer, R. *Pharm. Res.* **1994**, *11*, 1568. (h) Ding, J.; Liu, G. *Macromolecules* **1998**, *31*, 6554. (i) Donath, E.; Sukhorukov, G. B.; Caruso, F.; Davis, S. A.; Mohwald, H. *Angew. Chem., Int. Ed.* **1998**, *37*, 2202. (j) Thurmond, K. B., II; Kowalewski, T.; Wooley, K. L. *J. Am. Chem. Soc.* **1997**, *119*, 6656.

(2) (a) Pathak, C. P.; Sawhney, A. S.; Hubbell, J. A. *J. Am. Chem. Soc.* **1992**, *114*, 8311. (b) Gill, I.; Ballesteros, A. *J. Am. Chem. Soc.* **1998**, *120*, 8587.

(3) *Chem. Eng. News* **1999**, *77*, 32.

(4) Kmiec, E. B. *Am. Sci.* **1999**, *87*, 240.

(5) (a) Feilchenfeld, H.; Chumanov, G.; Cotton, T. M. *J. Phys. Chem.* **1996**, *100*, 4937. (b) Morris, C. A.; Anderson, M. L.; Stroud, R. M.; Merzbacher, C. I.; Rolison, D. R. *Science* **1999**, *284*, 622.

(6) (a) Zhao, M.; Sun, L.; Crooks, R. M. *J. Am. Chem. Soc.* **1998**, *120*, 4877. (b) Wendland, M. S.; Zimmerman, S. C. *J. Am. Chem. Soc.* **1999**, *121*, 1389.

(7) (a) Thurmond, K. B., II; Kowalewski, T.; Wooley, K. L. *J. Am. Chem. Soc.* **1997**, *119*, 6656. (b) Macknight, W. J.; Ponomarenko, E. A.; Tirrell, D. A. *Acc. Chem. Res.* **1998**, *31*, 781. (c) Harada, A.; Kataoka, K. *Science* **1999**, *283*, 65.

(8) (a) Hotz, J.; Meier, W. *Langmuir* **1998**, *14*, 1031. (b) Discher, B. M.; Won, Y.-Y.; Ege, D. S.; Lee, J. C−M.; Bates, F. S.; Discher, D. E.; Hammer, D. A. *Science* **1999**, *284*, 1143.
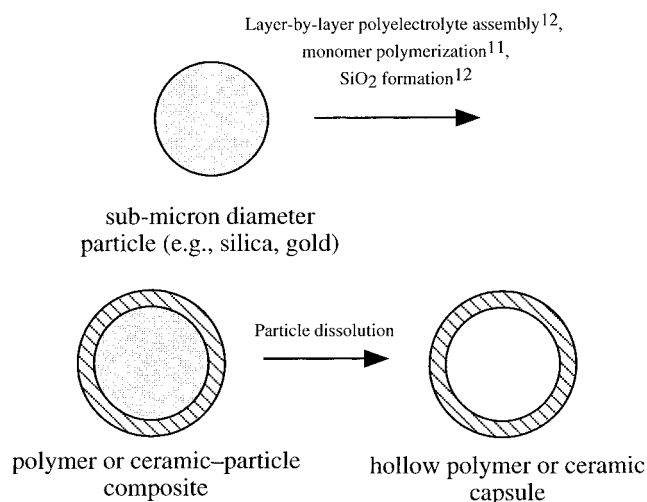
(9) Kataoka, K.; Miyazaki, H.; Bunya, M.; Okano, T.; Sakurai, Y. *J. Am. Chem. Soc.* **1998**, *120*, 12694.

(10) Martin, C. R.; Parthasarathy, R. V. *Adv. Mater.* **1995**, *7*, 487.

(11) (a) Marinakos, S. M.; Shultz, D. A.; Feldheim, D. L. *Adv. Mater.* **1999**, *11*, 34. (b) Marinakos, S. M.; Brousseau, L. C., III; Jones, A.; Feldheim, D. L. *Chem. Mater.* **1998**, *10*, 1214.

(12) (a) Giersig, M.; Ung, T.; Liz-Marzan, L. M.; Mulvaney, P. *Adv. Mater.* **1997**, *9*, 575. (b) Caruso, F.; Caruso, R. A.; Mohwald, H. *Science* **1998**, *282*, 1111.

Scheme 1

Figure 1. Transmission electron micrograph of ca. 30 nm diameter gold particles encapsulated in poly(pyrrole).

Scheme 2

template membrane.[10] Third, since nearly any small molecule or enzyme can be attached to gold particles,[13] this encapsulation scheme should prove to be entirely general.

Experimental Section

Chemicals. Gold nanoparticles were synthesized using $HAuCl_4$ and a citrate-reducing agent as described previously[11] or were purchased from Vector Labs. $HAuCl_4$, sodium citrate, $Fe(ClO_4)_3$, $NaBH_4$, KCN, $K_3[Fe(CN)_6]$, pyrrole, and *N*-methylpyrrole were purchased from Aldrich and used as received. Poly(vinylpyrrolidone) with $M_w = 40\,000$ was purchased from Acros.

Rhodamine B capped gold nanoparticles were synthesized by first exchanging mercaptoethylamine onto sulfonyl triphenylphosphine stabilized gold nanoparticles. This was accomplished by rapidly stirring sulfonyl triphenylphosphine (Aldrich; 1 mg/mL in H_2O) with 10 mL of gold sol. Rhodamine B isothiocyanate (Aldrich; 4.6 mg in 5 mL of ethanol) was then added to 10 mL of 0.3 nM nanoparticles. Reaction of isothiocyanate and amine moieties yielded gold nanoparticles containing an average of 15 000 covalently attached rhodamine B ligands, as determined by visible spectroscopy. Aluminum oxide membranes were purchased from Fisher Scientific.

Instrumentation. Transmission electron micrographs (TEM) were acquired on a Philips CM 12 electron microscope. Samples were prepared for analysis by placing several drops of the particle suspension on a Formvar-coated Cu grid (Ted Pella) and quickly wicking away the solvent with filter paper. To image hollow polymer capsules, a grid containing polymer−gold particle composites was dipped in 0.1 M KCN/0.001 M $K_3[Fe(CN)_6]$ gold etching solution for periods up to 5 min. Longer exposure completely removes the Formvar coating. UV−visible spectra were recorded with an HP 8450 diode array spectrophotometer.

Transport Measurements. All transport measurements were conducted on 30 nm diameter polymer-coated gold particles immobilized in porous Al_2O_3 membranes. Transport rates for $K_3[Fe(CN)_6]$/KCN (the "etchant solution") were measured by placing the membrane in a quartz cuvette, pipetting 1 mL of etchant into the cuvette, and monitoring the disappearance over time of the gold plasmon absorption at ca. 550 nm. Experiments on neutral poly(*N*-methylpyrrole) were performed by reducing poly(*N*-methylpyrrole-ClO_4)with aqueous $NaBH_4$ for at least 30 min prior to removing the gold particle.

Results and Discussion

This section is outlined as follows. First, the synthesis of polymer−gold particle composites and hollow polymer capsules

(13) (a) Keating, C. D.; Kovaleski, K. K.; Natan, M. J. *J. Phys. Chem. B* **1998**, *102*, 9414. (b) Dave, B. C.; Dunn, B.; Valentine, J. S.; Zink, J. I. In *Nanotechnology, Molecularly Designed Materials*; ACS Symposium Series 622; Chow, G.-M., Gonsalves, K. E., Eds.; American Chemical Society: Washington, DC, 1996.
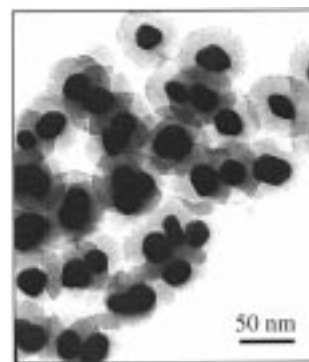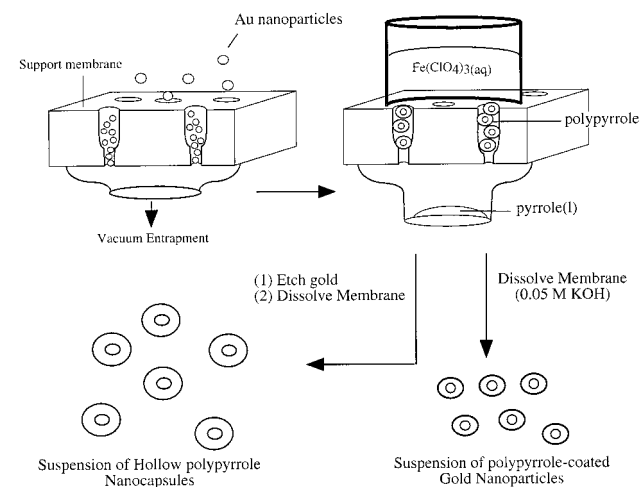
using a porous Al_2O_3 support membrane is described. Control over capsule core diameter, shell thickness, and multilayer sequence will be shown. The support membrane is strictly for convenience and is not involved chemically in the formation of polymer−gold particle composites. This will be illustrated with an entirely solution-phase method for synthesizing the same composites. Transport measurements of molecules through the polymer shell into the core as a function of polymer oxidation state are then described. Finally, the ability to load gold particles with an ω-terminated alkanethiolate, polymerize a capsule shell, and remove the gold to yield encapsulated guest molecules is illustrated with the cationic dye rhodamine B.

Membrane-Supported Synthesis of Hollow Nanocapsules. Membrane-supported methods for synthesizing polymer−gold particle composites are shown in Scheme 2. Briefly, gold nanoparticles (diameters from 5 to 200 nm) were first filtered into a porous Al_2O_3 support membrane (e.g., 200 nm diameter pore size). The solid support was then clamped in a glass tube, 0.1 M $Fe(ClO_4)_3$(aq) initiator was poured directly on top of the membrane, and several drops of neat monomer (e.g., pyrrole, *N*-methylpyrrole) were placed underneath the membrane. Monomer vapor diffused into the membrane, where it contacted initiator to form polymer. As shown in Figure 1, polymeric material deposits preferentially on the surface of gold particles to form hybrid gold core−polymer shell composites. Although our previous work has shown that spherical poly(pyrrole) nanoparticles will form in these membranes in the absence of gold particles,[11] we have found that with a relatively high loading of gold particles in the membrane (as determined qualitatively by the volume of particle suspension filtered through the membrane and by UV−visible spectroscopy) very
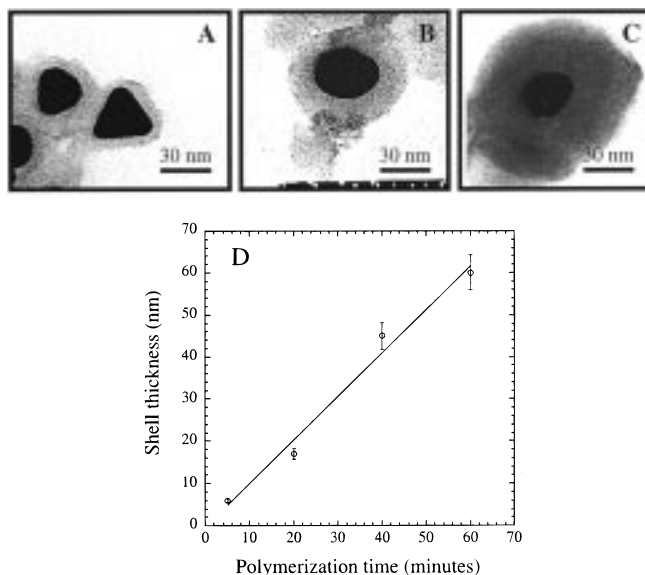
Figure 2. (A−C) Transmission electron micrographs of poly(pyrrole) shell thickness vs polymerization time: (A) 5 min; (B) 20 min; (C) 45 min. (D) Graphical representation of the microscopy data.
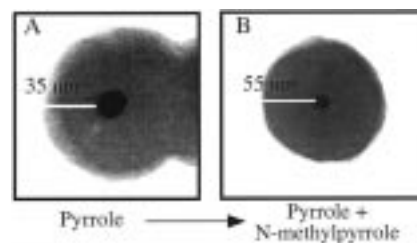

Figure 3. Transmission electron micrographs of poly(pyrrole)−gold particle composites formed with 15 min poly(pyrrole) deposition (A) and poly(*N*-methylpyrrole)/poly(pyrrole)/gold particle composites formed by sequentially depositing poly(pyrrole) for 10 min and poly(*N*-methylpyrrole) for 5 min (note that the magnifications are not identical in the two images).
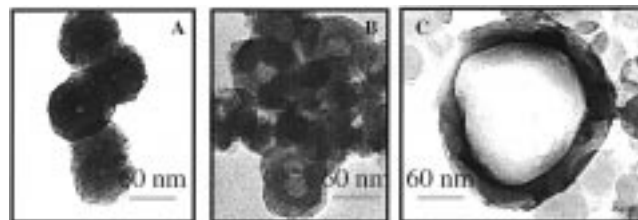

Figure 4. Transmission electron micrographs of hollow poly(pyrrole) capsules formed with 5 nm diameter (A), 30 nm diameter (B), and 200 nm diameter (C) gold template particles.

few polymer particles are found which do not contain a gold particle. Importantly, not a single gold particle which is not encapsulated in polymer has ever been observed by TEM. At this point the pyrrole monomer can be replaced in the cell with a second monomer (e.g., poly(*N*-methylpyrrole)) to grow multilayer composites, an aqueous solution containing $NaBH_4$ can be filtered through the membrane to reduce the polymer, or a gold etch solution consisting of 0.1 M KCN/0.001 M K_3-$[Fe(CN)_6]$ can be filtered through the membrane to remove the gold particle. In addition, the Al_2O_3 membrane may be dissolved with 0.05 M KOH(aq) at any time during these procedures to collect a solution suspension of composite particles or hollow polymer nanocapsules (Scheme 2). The significance of each of these treatments is discussed further below.

One consequence of the membrane-supported synthetic method is that it is extremely quick and easy to remove growing polymer−gold composites from the monomer vapor. This allows precise control over the thickness of the polymer skin. Figure 2A shows that, at short polymerization times (5 min), uniform polymer shells ca. 5 nm thick can be grown over 30 nm diameter gold template particles. Larger thicknesses are observed at longer polymerization times (20 min and 45 min in Figure 2B and 2C, respectively). The thickness measured for each of 20 particles from Figure 2C was found to lie between 18 and 22 nm (19.5 ± 1.4 nm). At polymerization times much longer than 60 min, the composite particles grow together to form long pseudo-one-dimensional strings of nanoparticles.[11]

The solid support also allows for quick removal of one monomer and the rapid introduction of a second monomer into the cell to form polymer multilayers. Figure 3 shows the results of such an experiment. Figure 3A is a TEM image after 15 min of poly(pyrrole) polymerization. The average shell thickness is 35 ± 1.8 nm. An identical gold-loaded support membrane treated with pyrrole for 15 min followed by *N*-methylpyrrole contains more polymer, as indicated by UV−visible spectroscopy (not shown), and has a much thicker shell 55 ± 3.9 nm (Figure 3B).

Conductive polymer−gold particle composites were converted to hollow polymer capsules by soaking a solid support membrane containing composite particles in an aqueous solution of 0.1 M KCN/0.001 M $K_3[Fe(CN)_6]$. Presumably, gold dissolution

occurs via transport of etchant species through the polymer shell to the core, where Au^0 is converted to $[Au(CN)_4]^-$. This is evidenced by a loss of the gold absorbance at ca. 550 nm (vide infra) and by the observation of a hollow core by TEM (Figure 4). Transport rates of the etch solution through the polymer shell are described further below. Here, we focus on the fact that the structural integrity of the capsule is maintained following gold dissolution. For example, Figure 4 shows TEM micrographs of hollow poly(pyrrole) capsules templated from 5, 30, and 200 nm diameter gold particles. The diameter of the resulting hollow capsule core is identical with that of the initial particle template. An imprint of the particle crystal facets is also clearly present in many capsules.

Solution-Phase Synthesis of Polymer−Gold Particle Composites. Although the solid-support method for synthesizing polymer−gold particle composites yields a material which is extremely easy to manipulate and characterize (vide infra), there would also be advantages of developing homogeneous solution-phase routes to polymer−nanostructure composites. For example, one might wish to grow thin skins of polymers on nanoscale materials that will not easily fit in a porous support membrane such as high aspect ratio metal nanowires or carbon nanotubes.

Solution-phase routes to polymer-coated nanostructures consist of combining an aqueous solution containing pyrrole (7.5 μL) and 10 nm diameter gold particles (2 mL) in 5 mL of H_2O with 10 mL of 0.1 M aqueous $Fe(ClO_4)_3$. Figure 5 shows TEM micrographs of poly(pyrrole)-coated gold particles synthesized using solution-phase methods. While every particle is again coated with polymer, we initially found substantial particle agglomeration (Figure 5A). This was prevented by adding 0.5 g of the steric stabilizer poly(vinylpyrrolidone) to the gold suspension. Figure 5B shows that agglomeration was indeed avoided in the presence of stabilizer.

Transport Rates of Gold Etchant into Conductive Polymer−Gold Particle Composites. A unique feature of conductive polymer nanocapsules is the possibility of effecting small molecule transport rates by switching the oxidation state of the
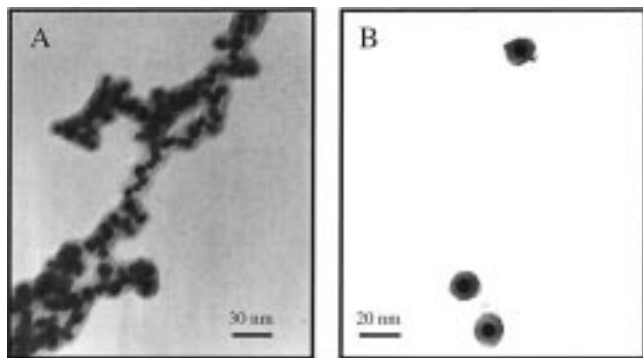
Figure 5. Transmission electron micrographs of poly(pyrrole)-coated gold nanoparticles synthesized using solution-phase methods (see text). (A) and (B) are composites synthesized in the absence and presence of poly(vinylpyrrolidone) stabilizer, respectively.

polymer. To characterize transport rates in poly(*N*-methylpyrrole) and poly(pyrrole) capsules, the gold plasmon absorption was monitored over time following exposure to the gold etch solution. Figure 6 shows that transport rates of etchant through poly(*N*-methylpyrrole)-coated gold nanoparticles depend on polymer oxidation state, those rates being faster for the neutral polymer. Similar data have been observed previously vis-à-vis gas and liquid transport in thick poly(*N*-methylpyrrole) films.[14] Those results were rationalized by considering the relative densities of neutral vs oxidized poly(*N*-methylpyrrole). Neutral poly(*N*-methylpyrrole) is known to contain a larger amount of void volume compared to oxidized poly(*N*-methylpyrrole),[15] a difference undoubtedly responsible for the transport rates seen here.

The data in Figure 6 were treated quantitatively using the following model for diffusion in a sphere:[16]

$$1 - (C_t - C_0)/(C_s - C_0) = b\exp(-At); \quad A = D\pi^2/L^2 \quad (1)$$

where C_t is the concentration of diffusing species at time t, C_s is surface concentration, C_0 is the diffusant concentration at the film/particle interface at $t = 0$, and b is a constant dependent on the initial boundary conditions employed in solving Fick's laws. Under these experimental conditions, C_0 may be set to 0 and the LHS of (1) may be related to the gold plasmon intensity. Thus

$$(abs_t/abs_0) = b\exp(-At) \quad (2)$$

where abs_0 and abs_t are the gold plasmon absorbances prior to etching and at some time t during etching, respectively.

Table 1 compares diffusion coefficients for gold etchant diffusing into conductive polymer capsules. The data fit eq 2 remarkably well ($R = 0.997$), considering the extinction coefficient of the gold particle is undoubtedly changing during the experiment (Figure 7). Diffusion coefficients are calculated to be roughly 3 times smaller through the oxidized polymer capsule vs the neutral capsule. This difference in diffusion rate is in fact diminished because the neutral poly(*N*-methylpyrrole) is partially redoped by the ferricyanide etchant. In addition,

(14) (a) Liang, W.; Martin, C. R. *Chem. Mater.* **1991**, *3*, 390. (b) Feldheim, D. L.; Elliott, C. M. *J. Membrane Sci.* **1992**, *70*, 9. (c) Feldhiem, D. L.; Krejcik, M.; Hendrickson, S. M.; Elliott, C. M. *J. Phys. Chem.* **1994**, *98*, 5714.

(15) Eisenberg, A.; Hird, B.; Moore, R. B., III. *Macromolecules* **1990**, *23*, 4098.

(16) (a) Crank, J.; Park, G. S. *Diffusion in Polymers*; Academic Press: New York, 1968. (b) Crank, J. *Mathematics of Diffusion*; Oxford University Press: London, 1956.
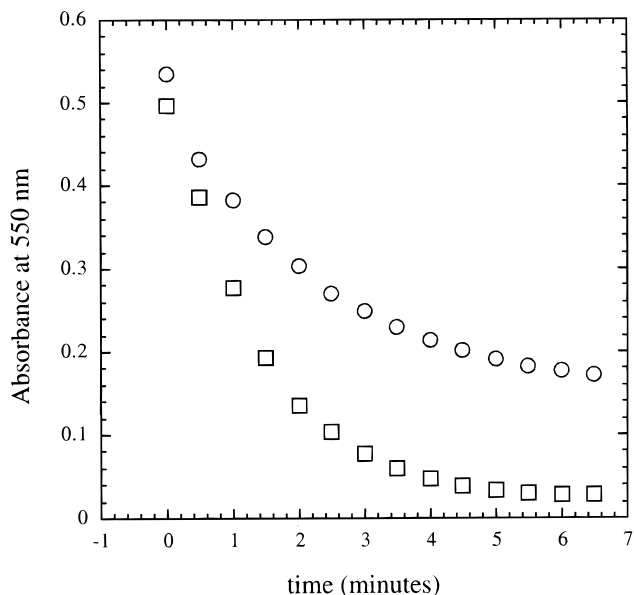

Figure 6. Absorbance of the gold template particle vs etch time for poly(*N*-methylpyrrole)-ClO$_4$ (○) and poly(*N*-methylpyrrole) (□).
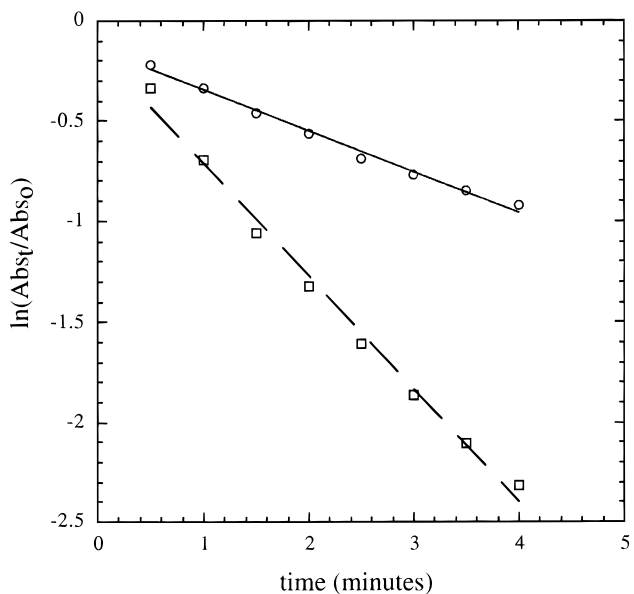

Figure 7. Fit of the etch data in Figure 6 to diffusion in a spherical polymer: (○) poly(*N*-methylpyrrole)-ClO$_4$; (□) poly(*N*-methylpyrrole). Diffusion coefficients of 5.0×10^{-12} and 1.5×10^{-11} cm^2/s, respectively, were calculated from the slopes.

Table 1. Diffusion Coefficients, D, for Various Polymer Nanocapsule Compositions

capsule composition	D (cm^2/s)
poly(*N*-methylpyrrole-ClO$_4$)	5.0×10^{-12}
poly(*N*-methylpyrrole)	1.5×10^{-11}
poly(pyrrole-ClO$_4$)	1.8×10^{-14}

diffusion through oxidized poly(pyrrole) is much slower compared to that through oxidized poly(*N*-methylpyrrole), a difference which can again be attributed to their relative porosities. Notably, the diffusion coefficients given in Table 1 agree well with those reported for other molecules diffusing through much thicker (micrometers) poly(pyrrole) and poly(*N*-methylpyrrole) films.[14]

Guest Entrapment. The focus of this study was whether particle-bound ligands are displaced from the gold surface upon
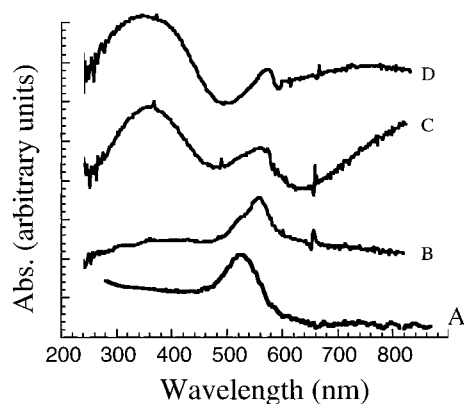
Figure 8. UV−visible spectra for 30 nm diameter gold particles (A), rhodamine B capped gold particles (B), poly(*N*-methylpyrrole)-encapsulated rhodamine B capped gold nanoparticles (C), and poly-(*N*-methylpyrrole)-encapsulated rhodamine B capped gold nanoparticles following exposure to gold etch solution.

polymer formation, or if they remain attached to the particle surface and are ultimately trapped inside the hollow polymer capsule following gold dissolution. Although, to our knowledge, rhodamine B has not been shown to have any desirable biological or catalytic activity, it was chosen as a guest because of its absorbance at ca. 556 nm, a region of relatively low absorptivity for poly(*N*-methylpyrrole). Figure 8 shows visible spectra for 30 nm diameter gold particles (Figure 8A), rhodamine B-capped gold (Figure 8B), poly(*N*-methylpyrrole)−rhodamine B composite particles (Figure 8C), and poly(*N*-methylpyrrole) capsules following gold etch (Figure 8D). Following polymer formation, absorptions for 30 nm diameter gold particles (ca. 545 nm shoulder), oxidized poly(*N*-methylpyrrole), *and* rhodamine B were observed, implying that polymer formation does not cause surface-bound ligands to desorb from the particle. The rhodamine B absorption peak is also clearly evident after removing the gold core.

Visible spectroscopy indicates that rhodamine B is present following polymer formation and gold core dissolution. However, it does not provide information on the location of rhodamine B in the nanoparticle. To address this question, rhodamine B loaded capsules were stained with aqueous CsOH for 48 h. Cs^+ is a known marker of carboxylic acid groups, rendering them visible by electron microscopy.[17] Figure 9 shows that rhodamine B remained in the hollow core following gold etching. No stain was observed in identical samples that were not loaded with rhodamine B.

In contrast to $K_3[Fe(CN)_6]$/KCN transport rates, which are relatively fast and are affected by the oxidation state of the

---

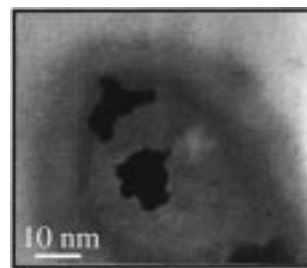(17) Ding, J.; Liu, G. *J. Phys. Chem. B* **1998**, *102*, 6107.

Figure 9. Transmission electron micrograph of poly(*N*-methylpyrrole)-encapsulated rhodamine B. The capsules were stained with aqueous CsOH to render the rhodamine B visible by electron microscopy.[17]

polymer shell, we found that rhodamine B was trapped inside the capsule for over 3 weeks, irrespective of polymer oxidation state. To test for a chemisorption mechanism compared to entrapment based on sterics, poly(*N*-methylpyrrole) capsules were soaked in rhodamine B (1 M in ethanol), rinsed, and immersed in pure ethanol. Visible spectra of the capsules revealed that rhodamine B was completely desorbed from the film within 24 h. These observations suggest that rhodamine B is trapped sterically within the poly(*N*-methylpyrrole) nanocapsules.

Conclusions

The synthesis and transport properties of poly(pyrrole)− and poly(*N*-methylpyrrole)−gold particle composite particles and hollow nanocapsules have been described. These synthetic methods enable excellent control over particle dimensions (e.g., shell thickness, hollow core diameter, and polymer sequence) and provide the ability to trap small molecules in the hollow capsule core. Extension of these methods to the entrapment of enzymes, proteins, DNA, and metal catalyst particles should be straightforward and are currently under investigation in our laboratories. Finally, although the biocompatability of poly-(pyrrole) has not been established previously, preliminary experiments have shown that T3 fibroblasts will ingest poly-pyrrole−gold composite particles without compromising subsequent T cell division.